

## **Cytochrome c Reduction by H<sub>2</sub>S Potentiates Sulfide Signaling**

Victor Vitvitsky<sup>1</sup>, Jan Lj. Miljkovic<sup>2,3</sup>, Trever Bostelaar<sup>1</sup>, Bikash Adhikari<sup>2,3</sup>, Pramod K. Yadav<sup>1</sup>,  
Andrea K. Steiger,<sup>4</sup> Roberta Torregrossa<sup>5</sup>, Michael D. Pluth<sup>4</sup>, Matthew Whiteman<sup>5</sup>, Ruma  
Banerjee<sup>1\*</sup> and Milos R. Filipovic<sup>2,3\*</sup>

<sup>1</sup>Department of Biological Chemistry, University of Michigan, Ann Arbor, MI 48109,

<sup>2</sup>Université de Bordeaux, IBGC, UMR 5095, F-33077 Bordeaux, France,

<sup>3</sup>CNRS, IBGC, UMR 5095, F-33077 Bordeaux, France,

<sup>4</sup>Department of Chemistry and Biochemistry, Institute of Molecular Biology, and Materials  
Science Institute, University of Oregon, Eugene, OR, USA,

<sup>5</sup>University of Exeter Medical School, St. Luke's Campus, Exeter, UK

Running Title: Cytochrome c reduction by H<sub>2</sub>S

\*Co-corresponding authors: milos.filipovic@ibgc.cnrs.fr or rbanerje@umich.edu

## Abstract

Hydrogen sulfide ( $\text{H}_2\text{S}$ ) is an endogenously produced gas that is toxic at high concentrations. It is disposed of by a dedicated mitochondrial sulfide oxidation pathway, which connects to the electron transfer chain at the level of complex III. Direct reduction of cytochrome C (Cyt C) by  $\text{H}_2\text{S}$  has been reported previously but not characterized. In this study, we demonstrate that reduction of ferric Cyt C by  $\text{H}_2\text{S}$  exhibits hysteretic behavior, which suggests the involvement of reactive sulfur species in the reduction process and is consistent with a reaction stoichiometry of 1.5:1.0 mole Cyt C reduced: $\text{H}_2\text{S}$  oxidized.  $\text{H}_2\text{S}$  increases  $\text{O}_2$  consumption by human cells (HT29 and HepG2) treated with the complex III inhibitor antimycin A, which is consistent with the entry of sulfide-derived electrons at the level of complex IV. Cyt C-dependent  $\text{H}_2\text{S}$  oxidation stimulated protein persulfidation in vitro while **silencing** of Cyt C expression decreased mitochondrial protein persulfidation in cell culture. Cyt C released during apoptosis was correlated with persulfidation of procaspase 9 and with loss of its activity. These results reveal a potential role for the electron transfer chain in general, and Cyt C in particular, for potentiating sulfide-based signaling.

H<sub>2</sub>S is an energy source for prokaryotes adapted for life in sulfide rich environments, but it is a potent respiratory toxin for other organisms. The targets of H<sub>2</sub>S poisoning are the metal centers in cytochrome c oxidase, the terminal station in the mitochondrial electron transfer chain (ETC).<sup>1,2</sup> At low concentrations however, H<sub>2</sub>S modulates physiological processes ranging from inflammation to cardiovascular function and apoptosis.<sup>3-5</sup> Cellular H<sub>2</sub>S levels must therefore be maintained within a nontoxic window by regulating enzymes involved in its biogenesis<sup>6-9</sup> and degradation.<sup>10,11</sup> The mitochondrial sulfide oxidation pathway transfers electrons from H<sub>2</sub>S oxidation to complex III via coenzyme Q.<sup>12</sup> In red blood cells lacking mitochondria, a non-canonical sulfide oxidation route uses ferric hemoglobin and catalyzes conversion of H<sub>2</sub>S to thiosulfate.<sup>13</sup> Polysulfides that are also produced in this reaction, are degraded by reductants such as glutathione.<sup>14</sup> Other heme proteins like myoglobin<sup>15</sup> and neuroglobin<sup>16</sup> also catalyze ferric heme-dependent H<sub>2</sub>S oxidation. Unlike hemoglobin and myoglobin, H<sub>2</sub>S oxidation by neuroglobin, in which the heme has two axial histidine ligands, does not involve direct coordination of sulfide to ferric iron.

Cytochrome c (Cyt C) resides in the mitochondrial intermembrane space and shuttles electrons between complexes III and IV in the ETC. Release of Cyt C into the cytosol triggers apoptotic activation of caspase 9.<sup>17</sup> As in neuroglobin, the heme in Cyt C **is 6-coordinate and** exhibits bis-His **or His/Met** ligation. In principle, electrons from the oxidation of H<sub>2</sub>S can enter the ETC at the level of complex IV either directly,<sup>18</sup> or indirectly via initial reduction of ferric Cyt C by sulfide.<sup>19</sup> However, the **standard redox potential** for the S<sup>•-</sup>, H<sup>+</sup>/HS<sup>-</sup> couple is +0.91 V (vs. NHE)<sup>20</sup> compared to +0.26 V for Cyt C,<sup>21</sup> rendering reduction of Cyt C by H<sub>2</sub>S thermodynamically unfavorable. Yet, reduction of Cyt C by sulfide has been observed *in vitro*,<sup>19,22</sup> and in the ciliated gills of *Guenkensia demissa*, a mussel that lives in sulfide-rich sediments.<sup>23</sup> An additional link between H<sub>2</sub>S and Cyt C was reported in a study on rotenone-induced apoptosis in which H<sub>2</sub>S exposure preserved mitochondrial function, limited Cyt C release, and inhibited dissipation of the mitochondrial proton membrane potential.<sup>24</sup> However, a quantitative analysis of H<sub>2</sub>S oxidation by Cyt C, identification of the

reaction products, and elucidation of its effects on apoptosis and persulfide signaling has been lacking.

In this study, we report the kinetics of Cyt C reduction by H<sub>2</sub>S, demonstrate formation of thiosulfate as a reaction product, and show stimulation of O<sub>2</sub> consumption in human cells treated with antimycin A, consistent with the delivery of electrons from H<sub>2</sub>S to complex IV via Cyt C. We also demonstrate that Cyt C in the presence of H<sub>2</sub>S stimulates protein persulfidation suggesting a potentiating role of the ETC in H<sub>2</sub>S-dependent signaling in general and in regulation of apoptosis via persulfidation of caspase 9 in particular.

## Results and Discussion

**Kinetics of Cyt C reduction by sulfide.** Addition of stoichiometric H<sub>2</sub>S to ferric Cyt C (Soret at 409 nm) results in its complete conversion to the ferrous form (415 nm) with sharpening of the  $\alpha/\beta$  bands at 550 and 520 nm (Fig. 1A). The kinetics of Cyt C reduction by sulfide exhibits a pronounced lag phase (Fig. 1B) indicating that either the reaction involves a slow step (e.g. ligand exchange from histidine to HS<sup>-</sup>) or that it is accelerated as H<sub>2</sub>S oxidation products accumulate. Cryo-ESI MS previously used to observe HS<sup>-</sup> coordination to ferric heme,<sup>15</sup> did not identify a comparable adduct with Cyt C (Supporting Fig. 1). The stoichiometry of the reduction reaction (1.5:1.0 Cyt C:sulfide) was independent of the presence of O<sub>2</sub> (Fig. 1 C). The Cyt C reduction rate showed a bell-shaped dependence on pH with a maximum at 7.5 and inflection points at  $6.7 \pm 0.1$  and  $8.5 \pm 0.1$  (Fig. 1D). Phosphate and citrate buffers, previously shown to bind Cyt C and influence its overall charge and redox potential,<sup>25</sup> significantly inhibited the rate of ferric Cyt C reduction by sulfide (not shown).

As discussed above, the one electron reduction of Cyt C with HS<sup>-</sup> is thermodynamically unfavorable, which could explain the observed lag phase (Fig. 1B). In principle, HS<sup>-</sup>/S<sup>•-</sup> could dimerize at a diffusion-controlled rate ( $k = 9 \times 10^9 \text{ M}^{-1} \text{ s}^{-1}$ )<sup>2</sup> giving HS<sub>2</sub><sup>-</sup> (eq 1). However, the probability of HS<sup>-</sup>/S<sup>•-</sup> reaching sufficiently high concentrations for the dimerization reaction

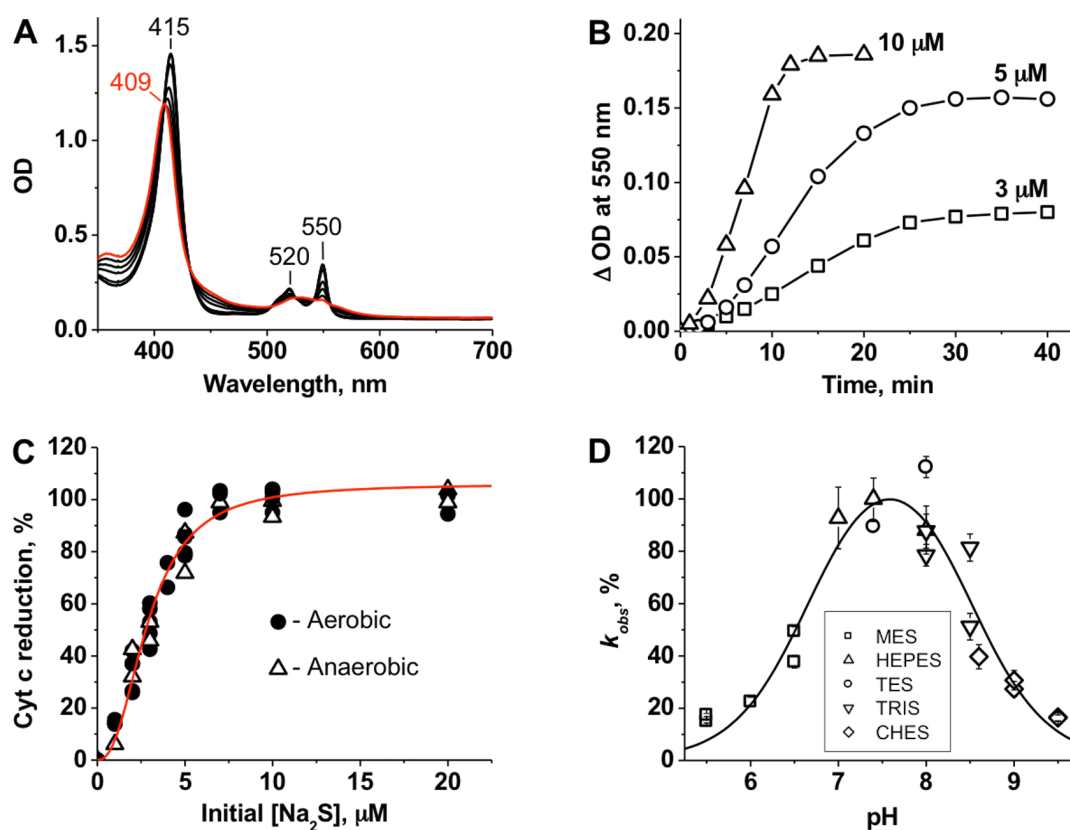
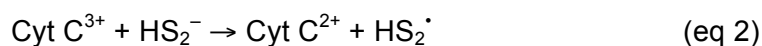


**Figure 1. Reduction of Cyt C by sulfide.** (A) The initial spectrum of ferric Cyt C (10  $\mu\text{M}$ ) in 100 mM HEPES buffer, pH 7.4 (red) shifts in the presence of 10  $\mu\text{M}$   $\text{Na}_2\text{S}$  (at 3, 5, 7, 10, 15, and 20 min, black lines) under aerobic conditions at 25  $^\circ\text{C}$ . (B) Kinetics of aerobic Cyt C reduction (10  $\mu\text{M}$ ) at 3, 5 and 10  $\mu\text{M}$   $\text{Na}_2\text{S}$  in 100 mM HEPES buffer, pH 7.4 at 25  $^\circ\text{C}$ . (C) Percent Cyt C (10  $\mu\text{M}$  in 100 mM HEPES buffer, pH 7.4) reduction as a function of sulfide concentration. The increase in absorbance at 550 nm was monitored after 1 h incubation with sulfide at 25  $^\circ\text{C}$  under aerobic or anaerobic conditions. The red line is a sigmoidal fit to the experimental data with  $S_{0.5} = 2.9 \pm 0.1 \mu\text{M}$  and  $n = 2.4 \pm 0.2$ . (D) The pH dependence of Cyt C reduction by sulfide. The rate of Cyt C (2.5  $\mu\text{M}$ ) reduction by sulfide (500  $\mu\text{M}$ ) was determined by anaerobic stopped-flow spectroscopy as described under Methods. The data are the mean  $\pm$  SD of 4 independent experiments as described under Methods. From the fit, estimates for  $\text{pK}_{a1}$  and  $\text{pK}_{a2}$  of  $6.7 \pm 0.1$  and  $8.5 \pm 0.1$ , respectively were obtained.

is likely to be low. Furthermore, formation of  $\text{HS}_2^-$  would not provide the driving force for Cyt C reduction, as the reaction (eq. 2) is thermoneutral ( $E^\circ'(\text{Cyt C}^{3+}/\text{Cyt C}^{2+}) = +0.26 \text{ V}$ ,  $E^\circ'(\text{S}_2^{2-}, \text{H}^+/\text{HS}_2^-) = +0.27 \text{ V}$ ).<sup>2,20</sup>

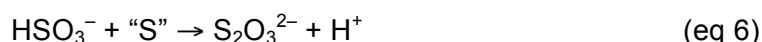


Alternatively, O<sub>2</sub> could react with the initially formed HS<sup>•</sup>/S<sup>•-</sup> at a diffusion-controlled rate ( $k = 5 \times 10^9 \text{ M}^{-1} \text{ s}^{-1}$ )<sup>2</sup> to produce SO<sub>2</sub><sup>•-</sup>, a strong reducing agent (eqs. 3-4). However, the extent of Cyt C reduction was independent of O<sub>2</sub> (Fig. 1C).



An alternative mechanism to explain the hysteretic behavior is that the initially formed HS<sup>•</sup>/S<sup>•-</sup> reacts with HS<sup>-</sup> ( $k_{on} = 4 \times 10^9 \text{ M}^{-1} \text{ s}^{-1}$ ,  $k_{off} = 5 \times 10^3 \text{ M}^{-1} \text{ s}^{-1}$ )<sup>2,20</sup> forming H<sub>2</sub>S<sub>2</sub><sup>•-</sup>, which is a strong reducing agent ( $E^{\circ'} (\text{HS}_2^{\bullet-}, \text{H}^+/\text{H}_2\text{S}_2^{\bullet-}) = -1.13 \text{ V}$ )<sup>2,20</sup> and could pull the Cyt C reduction reaction forward. Interestingly, Na<sub>2</sub>S<sub>2</sub> reduced Cyt C more rapidly than sulfide and without an observable lag phase (Fig. 2A).

**Degradation of excess sulfide in the presence of Cyt C.** Biphasic O<sub>2</sub> consumption kinetics were seen when Cyt C was mixed with excess sulfide (Fig. 2B). As the ratio of sulfide to Cyt C concentration was increased, the amplitude of the initial burst phase and the slope of the slow phase increased. This data is consistent with the model that the burst phase corresponds to the reduction of Cyt C during which the initially formed HS<sup>•</sup>/S<sup>•-</sup> is rapidly oxidized, while the slow phase represents subsequent oxidation reactions. The amplitude of the burst phase showed a hyperbolic dependence on sulfide concentration and asymptotically approached 0.7 equivalents of Cyt C to O<sub>2</sub> consumed (Fig. 2C). Biphasic O<sub>2</sub> consumption suggested formation of products with higher sulfur oxidation states. SO<sub>2</sub> formation (eq 4) would result in accumulation of sulfite, which in the presence of a sulfane sulfur donor ("S") would form thiosulfate as a final product (eq 5-6).<sup>2</sup>



We tested for the formation of sulfide oxidation products under aerobic conditions (Fig 2D). Loss of sulfide was paralleled by the accumulation of thiosulfate and to a lesser degree, sulfite. The recovery of sulfur **equivalents** in the thiosulfate, **which has two sulfur atoms**

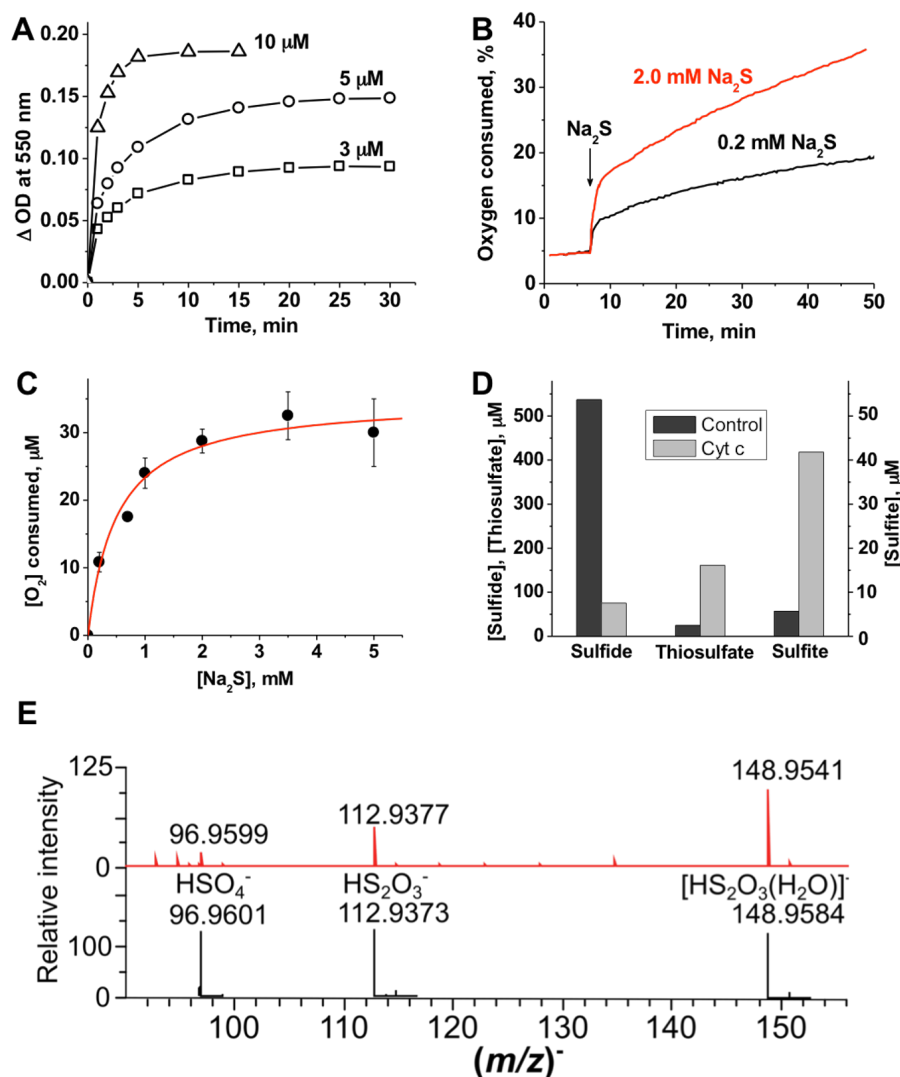


**Figure 2. Cyt C reduction kinetics and product analysis.** (A) Kinetics of aerobic Cyt C reduction (10  $\mu\text{M}$ ) in the presence of 3, 5 and 10  $\mu\text{M}$   $\text{Na}_2\text{S}_2$  in 100 mM HEPES buffer, pH 7.4 at 25  $^\circ\text{C}$ . Complete reduction with equimolar  $\text{Na}_2\text{S}_2$  was seen within 5-10 min. (B) Kinetics of  $\text{O}_2$  consumption in the presence of Cyt C and sulfide. Addition of sulfide to Cyt C (50  $\mu\text{M}$  in 100 mM HEPES buffer, pH 7.4) at 25  $^\circ\text{C}$  results in rapid initial consumption of  $\text{O}_2$  followed by a slower phase. (C) Dependence of the concentration of  $\text{O}_2$  consumed in the burst phase on sulfide concentration. A hyperbolic fit to the data (mean $\pm$ SD of 3-5 independent experiments) gives a  $K_{\text{act}}$  of  $0.5 \pm 0.1$  mM and a maximal  $\text{O}_2$  consumed of  $35 \pm 2$   $\mu\text{M}$  (red line) yielding a stoichiometry of 0.7:1.0 for  $\text{O}_2$  consumed:Cyt C. (D) Consumption of sulfide and accumulation of thiosulfate and sulfite 2 h after addition of 800  $\mu\text{M}$   $\text{Na}_2\text{S}$  to 100 mM HEPES buffer, pH 7.4 without (black bars) or with (gray bars) 100  $\mu\text{M}$  Cyt C at 25  $^\circ\text{C}$  under aerobic conditions. The initial levels of sulfide, thiosulfate, and sulfite were 756, 25, and 3.5  $\mu\text{M}$  respectively. (E) MS detection of sulfur products formed in the reaction of 10  $\mu\text{M}$  Cyt C with 100  $\mu\text{M}$   $\text{H}_2\text{S}$  in ammonium carbonate buffer, pH 7.7, under aerobic conditions. The reaction was monitored for 15 min at room temperature. The observed spectrum is at the top and the simulated spectra with isotopic distribution are below.

(~280  $\mu\text{M}$ ), and sulfite (40  $\mu\text{M}$ ) pools represent ~50% of the sulfide lost. Due to interference of Cyt C with the cold cyanolysis method, we were unable to evaluate the concentration of sulfane sulfur species in the reaction mixture. ESI-TOF MS in the negative mode confirmed formation of thiosulfate and also revealed the presence of sulfate (Fig. 2E). Although sulfite was not seen (possibly due to its low  $m/z$ ), we detected the sulfur trioxide radical anion  $\text{SO}_3^{\cdot-}$ , which increased in concentration with time (Supporting Fig. 2). Both  $\text{SO}_2^{\cdot-}$  and  $\text{H}_2\text{S}_2^{\cdot-}$  readily reduce  $\text{O}_2$  to form superoxide that can disproportionate to give  $\text{H}_2\text{O}_2$ .<sup>2,20</sup> The latter can oxidize ferrous Cyt C, enabling its redox cycling.<sup>26,27</sup> Sulfite, peroxide and heme proteins are known to produce  $\text{SO}_3^{\cdot-}$  which is a potent oxidant that is proposed to play a role under certain pathological conditions.<sup>28-30</sup>  $\text{SO}_3^{\cdot-}$  could also contribute to Cyt C re-oxidation to establish a pseudo-catalytic cycle for  $\text{H}_2\text{S}$  removal.

**Cyt C stimulates *in vitro* protein persulfidation.** Protein thiols represent a potentially large pool of intracellular  $\text{HS}^{\cdot}/\text{S}^{\cdot-}$  scavengers (eq 7). To test the hypothesis that protein thiols are



sinks for  $\text{HS}^{\cdot}/\text{S}^{\cdot-}$ , we first used time-resolved ESI-TOF-MS to monitor a reaction mixture containing Cyt C,  $\text{H}_2\text{S}$  and cysteine. Formation of cysteine persulfide (as  $[\text{CysSSH} + \text{H}]^+$  and  $[\text{2CysSSH} + \text{H}]^+$  ions) and its decay products  $\text{CysSSCys}$  (Fig. 3A) and  $\text{CysSSSCys}$  (Supporting Fig. 3A) was observed. While formation of  $\text{CysSSH}$  plateaued within 1 min, formation of  $\text{CysSSCys}$  continued (Fig. 3B, Supporting Fig. 3B) supporting our previous report of the lability of  $\text{CysSSH}$ .<sup>31</sup>

Next, we tested Cyt C-dependent persulfidation of a model protein, human serum albumin (HSA). We have previously shown that addition of water-soluble heme iron and  $\text{H}_2\text{S}$  triggers protein persulfidation.<sup>32</sup> Incubation of HSA with sulfide in the presence of Cyt C also resulted in protein persulfidation (detected using the  $\text{Cy3-CN}$ -based tag switch method)<sup>33</sup> that was proportional to the concentration of Cyt C (Fig. 3C). In contrast, when Cyt C was replaced with myoglobin, which oxidizes sulfide to polysulfides and thiosulfate via an inner



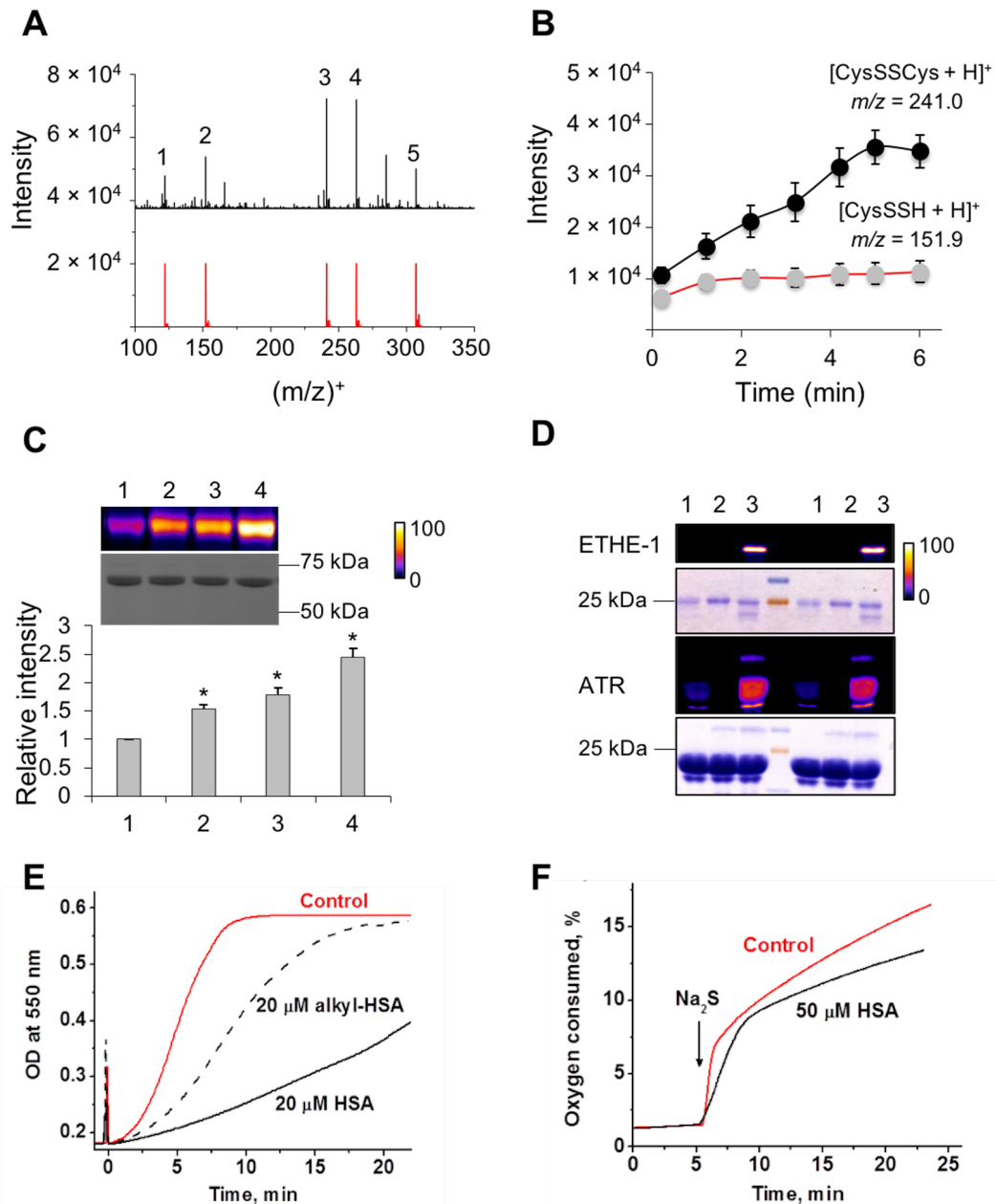
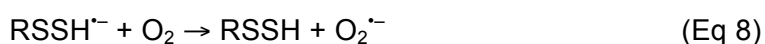


**Figure 3. Cyt C stimulates  $H_2S$ -dependent persulfidation.** A) Mass spectrum of the reaction mixture ( $t = 6$  min) containing  $20 \mu M$  Cyt C,  $100 \mu M$   $H_2S$  and  $200 \mu M$  cysteine in ammonium carbonate buffer pH 7.7,  $21^\circ C$ , and simulated isotopic distributions for some of the identified species: 1-  $[CysSH + H]^+$ , 2-  $[CysSSH + H]^+$ , 3-  $[CysSSCys + H]^+$ , 4-  $[CysSSCys + Na]^+$ , 5-  $[2CysSSH + H]^+$ . B) Kinetics of  $[CysSSH + H]^+$  ( $m/z = 151.9$ ) and  $[CysSSCys + H]^+$  ( $m/z = 241.0$ ) formation. Data represent mean  $\pm$  SD of 3 independent experiments. C) Persulfidation of HSA ( $10 \mu M$ ) in PBS pH 7.4, incubated for 30 min at room temperature with  $500 \mu M$   $Na_2S$  (lane 1) and  $2 \mu M$  (lane 2),  $20 \mu M$  (lane 3) and  $200 \mu M$  (lane 3) Cyt C. Data represent the mean  $\pm$  SD;  $n=3$ ,  $*p<0.001$ . D) Persulfidation of purified ( $1 \mu M$ ) ETHE-1 and ( $10 \mu M$ ) ATR treated with either  $100 \mu M$   $H_2S$  (lane 1),  $10 \mu M$  Cyt C (lane 2) or combination of both (lane 3). The results of two separate experiments are shown in the figure. Persulfidation (C-D) was detected by the CN-Cy3-based tag switch method (upper panels) while equal loading was detected by Coomassie blue staining (lower panels). The gel was artificially colored using ImageJ to enhanced visualization of changes and the

fluorescence intensity scale is provided on the right. The persulfidation procedure is described in Supporting Materials and Methods. E) Aerobic kinetics of Cyt C (20  $\mu$ M in 100 mM HEPES buffer, pH 7.4 at 25  $^{\circ}$ C) reduction (monitored at 550 nm) by Na<sub>2</sub>S (20  $\mu$ M)  $\pm$  untreated or alkylated HSA (20  $\mu$ M). Sulfide was added at time 0. F) Kinetics of O<sub>2</sub> consumption after addition of 0.2 mM Na<sub>2</sub>S to ferric Cyt C (50  $\mu$ M in 100 mM HEPES buffer, pH 7.4)  $\pm$  50  $\mu$ M HSA at 25  $^{\circ}$ C.

sphere electron transfer mechanism, an increase in persulfidation was not observed (Supporting Fig. 4). The residual persulfidation signals seen in the control lanes result from H<sub>2</sub>S-induced reduction of the disulfide bond in HSA. We also demonstrated that the human mitochondrial proteins, ETHE-1 and adenosyltransferase (ATR), previously identified as persulfidation targets, were also persulfidated by Cyt C/H<sub>2</sub>S (Fig. 3D).

Interception of reactive sulfur species (HS<sup>•</sup>/S<sup>•-</sup>) by cysteine residues on proteins should decrease the rate of Cyt C reduction by H<sub>2</sub>S and O<sub>2</sub> consumption. A substantial decrease in the rate of Cyt C reduction was in fact observed in the presence of equimolar HSA, which was attenuated by prior alkylation of HSA cysteines with iodoacetamide (Fig. 3E). HSA also decreased the rate of O<sub>2</sub> consumption impacting both the burst and slow phases of the reaction (Fig. 3F). Interestingly, the amplitude of the burst phase was increased in the presence of HSA. The initially formed RSSH<sup>•-</sup> protein radical anion is expected to be a strong reducing agent in analogy with RSSR<sup>•-</sup> ( $E^{\circ}$  (RSSR/RSSR<sup>•-</sup>) = -1.4 V).<sup>34</sup> Since outer sphere electron transfer from the protein radical to Cyt c is likely to be precluded by steric hindrance, O<sub>2</sub> would be the only available electron acceptor (eq 8), which could explain the higher amplitude observed for the burst phase (Fig. 3F).



**Cyt C silencing decreases intracellular persulfidation.** To further investigate its role in protein persulfidation, Cyt C was silenced in HeLa cells. Under normoxic conditions, Cyt C silencing resulted in a small but statistically significant decrease in endogenous protein persulfidation as detected by the CN-Cy3-based tag switch method (Fig. 4A). The mitochondria-targeted H<sub>2</sub>S donor AP39 caused a large increase in protein persulfidation as

seen previously,<sup>33</sup> which was reduced by Cyt C siRNA treatment. The perinuclear localization of the persulfidation signal in AP39-treated cells confirms mitochondrial localization as reported for this donor.<sup>33,35,36</sup>

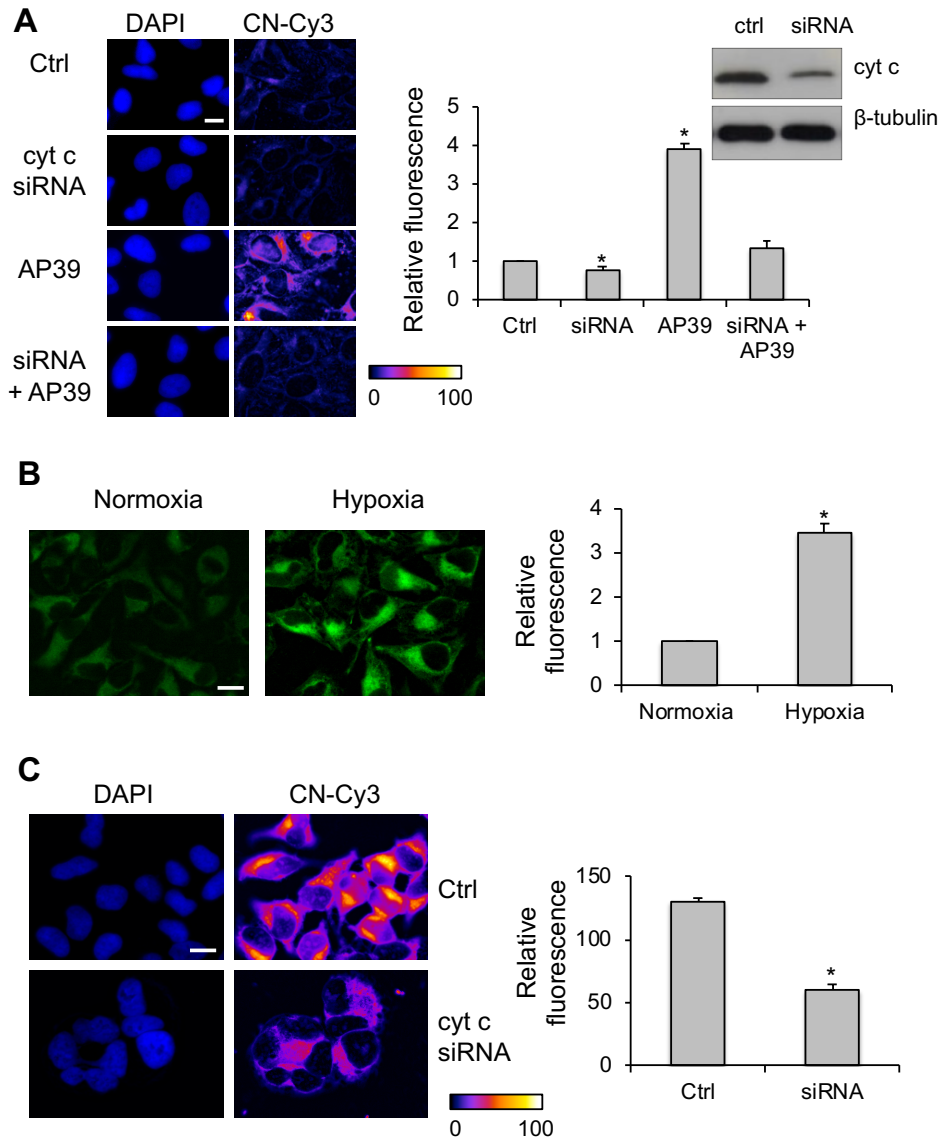


**Figure 4. Cyt C silencing decreases protein persulfidation.** (A) Under normoxic conditions, silencing of Cyt C in HeLa cells (confirmed by Western-blot analysis) led to a small but measurable decrease in basal persulfidation levels, which was increased by the mitochondria-targeted H<sub>2</sub>S donor, AP39 (200 nM). Scale bar 5  $\mu$ m. (B) Exposure of HeLa cells to hypoxia for 1 h results in increased endogenous H<sub>2</sub>S levels as detected by MeRho-Az. Scale bar 10  $\mu$ m. (C) Under hypoxic conditions, the levels of protein persulfidation are high but significantly reduced by Cyt C silencing. Scale bar 10  $\mu$ m. Representative microscopy images are given on the left and quantitative image analysis on the right. The results represent average fluorescence intensity (F. I.) detected from  $n \geq 40$  cells  $\pm$  SEM of 5 independent images. \* $p < 0.001$ .

H<sub>2</sub>S oxidation is dependent on the presence of a functional ETC and lower O<sub>2</sub> levels lead to H<sub>2</sub>S accumulation.<sup>37</sup> Using MeRho-Az, a bright fluorescence probe for H<sub>2</sub>S detection,<sup>35</sup> we observed a substantial increase in intracellular H<sub>2</sub>S in HeLa cells exposed to <5% O<sub>2</sub> (Fig. 4B). A significant increase in protein persulfidation was observed in cells exposed to hypoxic conditions, which was diminished by silencing Cyt C (Fig. 4C).

**Sulfide stimulates O<sub>2</sub> consumption in complex III-inhibited cells.** To assess whether electrons from sulfide oxidation can bypass complex III and enter at the level of complex IV (Fig. 5A), the O<sub>2</sub> consumption rate (OCR) was assessed with human cells in suspension. The OCR decreased to 2.5% (HepG2) and 5% (HT29) of the initial values in the presence of antimycin A, a complex III inhibitor (Fig. 5B,C). Addition of sulfide (20 μM) increased OCR by an average of 30% (HT29) and 95% (HepG2) above the antimycin-treated value. Higher concentrations of sulfide (100 μM) inhibited O<sub>2</sub> consumption as expected, presumably due to inhibition of complex IV. Addition of KCN, which poisons complex IV, blocked OCR confirming that O<sub>2</sub> consumption induced by sulfide was linked to mitochondrial respiration.

Next, we assessed how inhibition of complex III and IV affects persulfidation in functional mitochondria that should produce H<sub>2</sub>S *via* the action of 3-mercaptopyruvate sulfurtransferase. Purified yeast mitochondria (*Saccharomyces cerevisiae*) treated with antimycin A showed an increase in intra-mitochondrial protein persulfidation, an effect that was inhibited by KCN (Fig. 5D). This is in accordance with our hypothesis that even when H<sub>2</sub>S oxidation is inhibited by antimycin A, Cyt C-dependent consumption of H<sub>2</sub>S can still occur, leading to increased protein persulfidation. Inhibition of cytochrome C oxidase (by KCN) on the other hand, would prevent reoxidation of Cyt C and stop the cycle (Fig. 5D).

Collectively, these results suggest that the canonical sulfide oxidation pathway can be bypassed to some extent by direct reduction of Cyt C. The reactive sulfur species formed

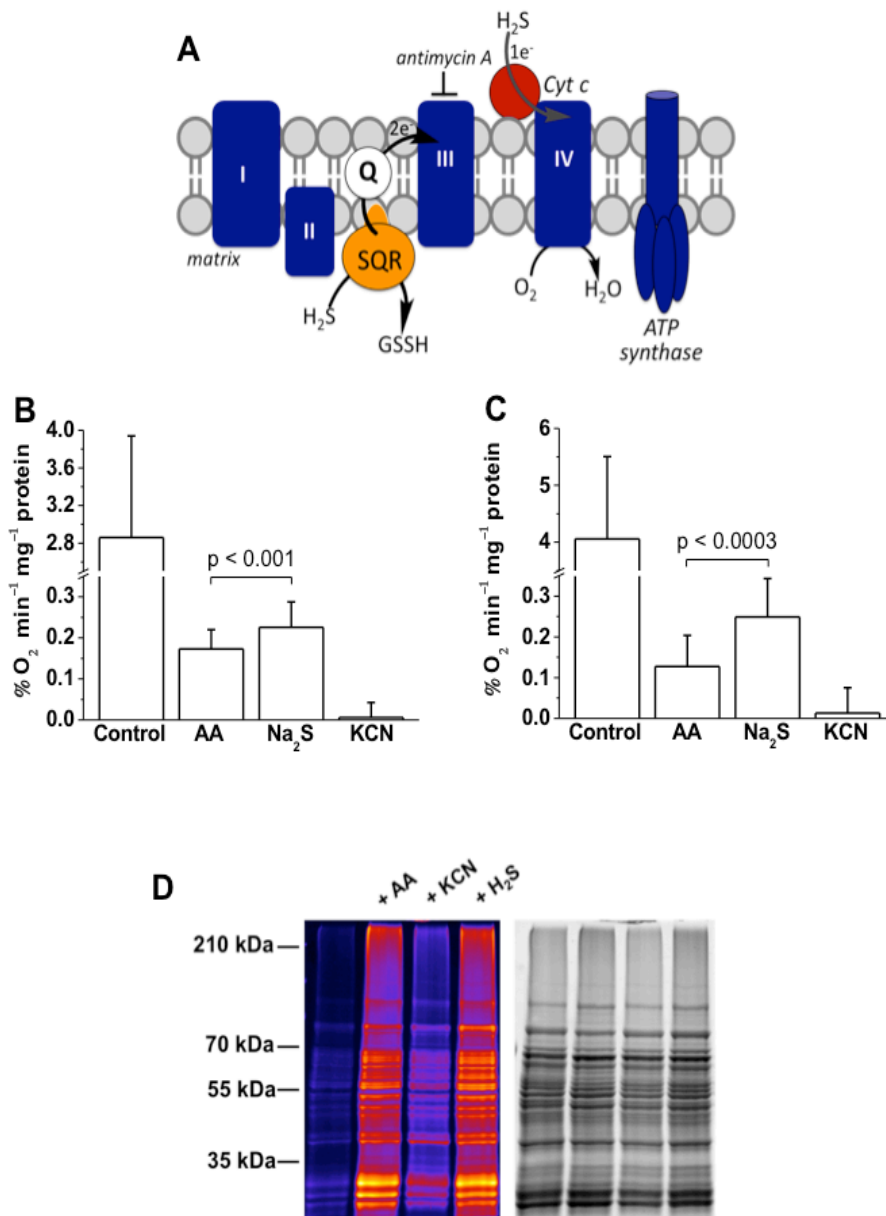


**Figure 5.** Sulfide stimulates O<sub>2</sub> consumption by mammalian cells and controls persulfidation of mitochondrial proteins. (A) Cartoon showing electrons from H<sub>2</sub>S oxidation enter the ETC at the level of complex III via the reduced quinone pool. Entry into complex IV via Cyt C can be monitored in the presence of antimycin A, a complex III inhibitor. (B and C) O<sub>2</sub> consumption rates of HT29 (B) and HepG2 (C) cells before (control) and after treatment with 2 μg ml<sup>-1</sup> antimycin A (AA) followed by 20 μM Na<sub>2</sub>S. Finally, antimycin A-treated cells were exposed to 5 mM KCN. The data are the mean±SD of 12 (B) or 6 (C) independent experiments; p value shows the statistical significance for the difference between antimycin A ± sulfide treated cells. D) Protein persulfidation in purified mitochondria is affected by ETC. Functional mitochondria were isolated from *S. cerevisiae* and preincubated with 2.5 μg ml<sup>-1</sup> antimycin A or 10 mM KCN for 10 min at 37 °C or treated with 1 μM H<sub>2</sub>S for 20 min at 37 °C. Persulfidation was monitored by improved tag-switch method. First lane represents the basal persulfidation level in untreated functional mitochondria. Total protein load is shown in the gel on the right.

under these conditions can react with protein thiols increasing persulfidation. We speculate that this situation could be particularly important in ischemia/reperfusion, protecting proteins from ROS-induced hyper-oxidation during the reperfusion phase.

**Cyt C-induced persulfidation controls caspase 9 activity.** In addition to its role in mitochondrial energy metabolism, Cyt C is an important regulator of apoptosis following its release into the cytosol.<sup>38,39</sup> In the presence of Cyt C, apoptotic protease activating factors in the apoptosome activate procaspase 9, triggering a protease cascade.<sup>40</sup> Due to this functional association with Cyt C, we tested whether caspase 9, a cysteine protease, is persulfidated in the presence of H<sub>2</sub>S and Cyt C. Incubation with Cyt C and H<sub>2</sub>S stimulated persulfidation of recombinant murine procaspase 9 (Fig. 6A). Next, we assessed caspase 9 activity in HeLa cell extracts using the fluorogenic caspase-9 substrate. Cyt C significantly stimulated caspase 9 activity, which was **diminished** in the presence of sulfide (Fig. 6B).

Activity of caspase 9 in intact cells was also assessed by flow cytometry in Jurkat cells treated with staurosporine, an apoptosis inducer.<sup>41</sup> Staurosporine induced caspase 9 activity (Fig. 6C), which was prevented by the slow-releasing H<sub>2</sub>S donor, 100 μM GYY4137. In contrast, the faster-releasing H<sub>2</sub>S donor, ammonium tetrathiomolybdate, only partially inhibited the effect of staurosporine on caspase activation (Fig. 6C).

Procaspase 3 is the downstream target of caspase 9, which cleaves it to the active caspase 3 form.<sup>42</sup> Induction of apoptosis by antimycin A treatment of HeLa cells for 16 h resulted in the expected increase in caspase 3 activity, which was partially inhibited by pre-incubating the cells for 2h with GYY4137 (Fig. 6D).

Finally, we checked whether persulfidation of procaspase 9 was affected in HeLa cells treated with staurosporine for 6 h. Cells were either pre-treated with GYY4137 prior to staurosporine addition or treated for 2h after induction of apoptosis by staurosporine (Supporting Fig. 5A). GYY4137 treatment decreased total procaspase 9 levels (Fig. 6E). Persulfidation of procaspase 9 was however significantly increased when the cells were treated with both staurosporine and the H<sub>2</sub>S donor (Fig. 6E, Supporting Fig. 5B).

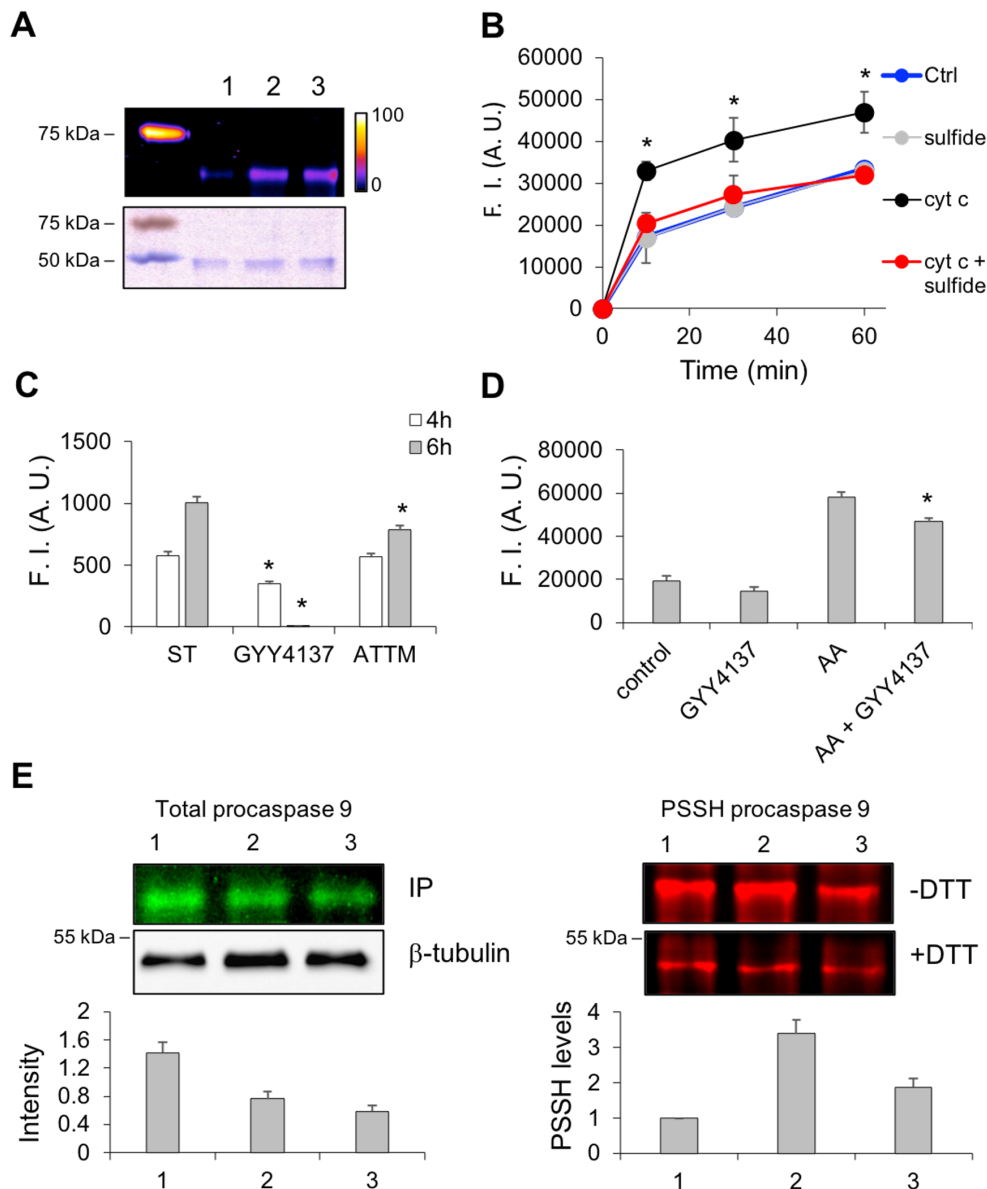


**Figure 6. Cyt C-mediated procaspase 9 persulfidation and activity.** (A) Murine recombinant procaspase 9 (1  $\mu$ M) was incubated with 5  $\mu$ M H<sub>2</sub>S for 30 min at 37 °C in the absence (lane 1) or presence of 0.5 (lane 2) and 2  $\mu$ M (lane 3) Cyt C. Persulfidation was detected by the CN-Cy3-based tag switch method (*upper panel*) while equal loading was confirmed by Coomassie blue staining (*lower panel*). (B) H<sub>2</sub>S inhibits Cyt C-induced caspase 9 activation in cell lysates. Cyt C (500 nM) was added to freshly prepared HeLa cell lysates and caspase 9 activity was monitored using a fluorescence caspase 9 kit. Simultaneous addition of Cyt C and H<sub>2</sub>S (10  $\mu$ M) inhibited the Cyt C-induced increase in fluorescence. (C) Cyt C-induced caspase 9 activation in Jurkat cells is inhibited by H<sub>2</sub>S donors. Apoptosis was induced by staurosporine (ST, 2.5  $\mu$ M) and caspase 9 activity was monitored by flow cytometry using the caspase 9 FITC Staining Kit 4 and 6 h after induction. Treatment of cells with (GY4137, 100  $\mu$ M) or ammonium tetrathiomolybdate (ATTM, 200  $\mu$ M) reduced fluorescence. (D) Inhibition of caspase 3 activation in cells treated with antimycin A and the slow-releasing H<sub>2</sub>S donor, GY4137 (100  $\mu$ M). HeLa cells were incubated with antimycin A (300  $\mu$ M) overnight to induce Cyt C release from mitochondria. GY4137 when used, was

added 2 h prior to antimycin A. Caspase 3 activity was monitored in cell lysates as described in B. E) Persulfidation of procaspase 9 in HeLa cells treated with 2.5  $\mu$ M ST (1) that were either pretreated for 2 h (2) or treated for the last 2 h (3) with GYY4137 (100  $\mu$ M). (Left) Total procaspase 9 levels. (Right) Persulfidation (PSSH) levels of procaspase 9. PSSH levels were quantified by measuring the difference in fluorescence between DTT treated and untreated samples and normalizing this to the total procaspase 9 levels. The strategy used for sample processing to detect total versus persulfidated procaspase 9 is explained in Supporting Information and Supporting Fig. 5.

Several caspases, including caspase 9 are inhibited by S-nitrosation of the active site cysteine.<sup>43,44</sup> Several mechanisms have been proposed to explain the antiapoptotic effects of sulfide.<sup>45,46</sup> We provide evidence that reactive sulfur species generated by Cyt C mediated H<sub>2</sub>S oxidation can tag proteins with the cysteine persulfide modification. We posit that this reactivity might be enhanced under hypoxic conditions when H<sub>2</sub>S oxidation is inhibited, or under apoptotic conditions when Cyt C is released into the cytoplasm and is disconnected from its mitochondrial electron donors e.g. complex III. If H<sub>2</sub>S synthesis is upregulated under these conditions, persulfidation of protein targets in the proximity of Cyt C like procaspase 9, will result. Inhibition of caspase 9 activity by persulfidation opens up the possibility of designing peptidomimetic persulfide donors to inhibit its activity, similar to the reported S-nitrosothiol containing peptide.<sup>47</sup>

In summary, we propose that the reaction between Cyt C and H<sub>2</sub>S results in the initial formation of a HS<sup>•</sup>/S<sup>-</sup> radical. In a cellular milieu, HS<sup>•</sup>/S<sup>-</sup> could suffer one of at least two fates: (i) be trapped by proteins, forming protein persulfides and superoxide, or (ii) be trapped by oxygen forming HSO<sub>2</sub><sup>•</sup> (Fig. 7). Dismutation of superoxide generated in (i) would give H<sub>2</sub>O<sub>2</sub>, which together with H<sub>2</sub>S, could lead to more persulfidation.<sup>48</sup> Formation of HSO<sub>2</sub><sup>•</sup> in (ii) could further facilitate Cyt C reduction, resulting in sulfite and thiosulfate production. Cyt C reduction by H<sub>2</sub>S can fuel the ETC, bypassing complex III. Oxidation of Cyt C by complex IV would allow it to cycle between sulfide and the ETC, potentially leading to accumulation of reactive sulfur species. Cyt C-assisted protein persulfidation might represent a previously unrecognized source of reactive sulfur species that mediates the protective effects attributed to protein persulfidation.



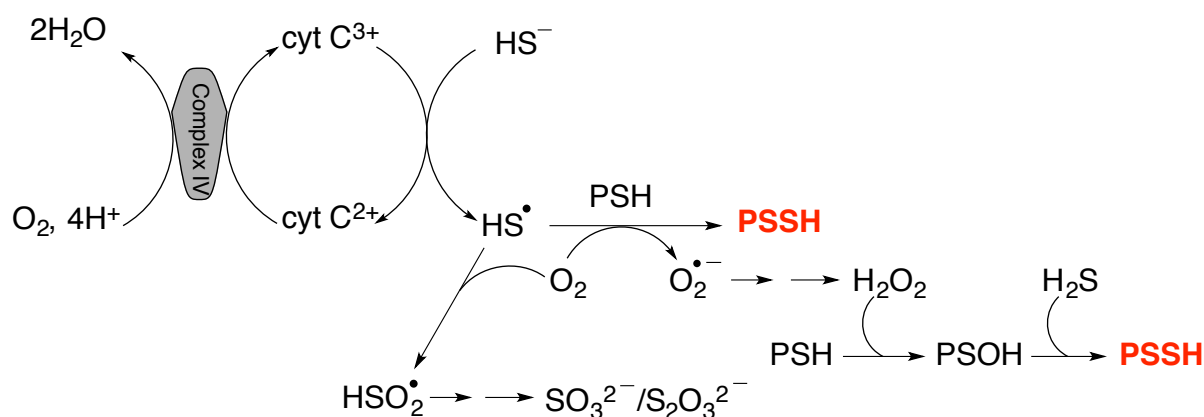


**Figure 7. Protein persulfidation catalyzed by cyt C/H<sub>2</sub>S couple.**

## Methods

**Reagents.** Antimycin A, equine heart ferric Cyt C, HSA, iodoacetamide and Na<sub>2</sub>S nonahydrate (99.99%) were purchased from Sigma Aldrich. Sodium disulfide (Na<sub>2</sub>S<sub>2</sub>) was from Dojindo Molecular Technologies, monobromobimane FluoroPure grade was from Molecular Probes (Grand Island, NY). GYY4137, AP39 and MeRho-Az were synthesized in-house as described, respectively<sup>35,36,49</sup>. 2-(methylsulfonyl)-1,3-benzothiazole was from Santa Cruz Biotechnology and CN-Cy3 synthesized as reported previously.<sup>33</sup> Murine procaspase 9 was from Enzo Life Science. The siRNA for Cyt C was purchased from Santa Cruz Biotechnology. For the anaerobic experiments, buffers were purged with argon. To maintain high purity, Na<sub>2</sub>S solutions were made in an argon box by dissolving solid Na<sub>2</sub>Sx9H<sub>2</sub>O into argon purged water, as recommended<sup>2,19</sup>.

**Cell culture.** Human colon cancer (HT29), hepatocellular carcinoma (HepG2), cervical cancer (HeLa) and immortalized human T-lymphocyte (Jurkat) cell lines were purchased from ATCC. Cells were cultured in 10 cm plates in EMEM (HepG2) or RPMI 1640 (HT29) medium supplemented with 10% FBS (Gibco) and 1% penicillin (10,000 U ml<sup>-1</sup>)/streptomycin (10000 µg ml<sup>-1</sup>) mixture (Gibco). Jurkat and HeLa cells were cultured in 75 cm flasks in complete RPMI medium or DMEM (Sigma Aldrich) respectively, supplemented

with 10% FBS and 1% penicillin (10,000 U ml<sup>-1</sup>)/streptomycin (10000 µg ml<sup>-1</sup>) mixture (Sigma Aldrich).

Detailed description of the methods is given in supporting information.

**Acknowledgment.** This work was supported by the French State in the frame of the "Investments for the future" Programme IdEx Bordeaux, reference ANR-10-IDEX-03-02 and by ATIP-AVENIR grant (to M. R. F.), National Institutes of Health (GM112455 to R. B; R01GM113030 to MP), the Medical Research Council, UK (MR/M022706/1 to MW), the National Science Foundation (DGE-1309047 to AS), and the Brian Ridge Scholarship (RT). The authors are grateful to Marie-France Giraud (IBGC) for the help with mitochondria purification.

**Conflict of Interest:** MW has patents on the therapeutic and agricultural use of mitochondria-targeted, and other, hydrogen sulfide delivery molecules.

**Author contributions:** VV – design of experiments, spectral analysis of Cyt C interaction with sulfide and hydrodisulfide, pH dependence of Cyt C reaction with sulfide, oxygen consumption assays, data analysis, writing manuscript; JLJM – performed experiments with Cyt C siRNA, with fluorescence microscopy, caspase activity, flow cytometry, mitochondrial persulfidation, data analysis, writing manuscript; TB–oxygen consumption assays with Cyt C, data analysis, writing manuscript; BA – fluorescence microscopy, H<sub>2</sub>S measurements, HSA persulfidation; PKY - performed and analyzed the stopped-flow kinetic studies; AS, MP, RT, MW – contributed new analytical tools and MP and MW co-wrote the manuscript. RB – helped design kinetic, spectroscopic and OCR experiments, analyzed the data and co-wrote the manuscript; MRF – design of experiments, mass spectrometry, persulfidation of ATR and ETHE1, data analysis, writing manuscript.

*Supporting Information Available:* This material is available free of charge *via* the Internet.

## References

- (1) Keilin, D. Cytochrome and Respiratory Enzymes. *Proc. R. Soc. London. Ser. B, Contain. Pap. a Biol. Character* **1929**, *104* (730), 206–252.
- (2) Filipovic, M. R.; Zivanovic, J.; Alvarez, B.; Banerjee, R. Chemical Biology of H<sub>2</sub>S Signaling through Persulfidation. *Chemical Reviews*. 2018, pp 1253–1337.
- (3) Kimura, H. Hydrogen Sulfide: From Brain to Gut. *Antioxid. Redox Signal.* **2010**, *12* (9), 1111–1123.
- (4) Kabil, O.; Banerjee, R. Redox Biochemistry of Hydrogen Sulfide. *J. Biol. Chem.* **2010**, *285* (29), 21903–21907.
- (5) Kabil, O.; Motl, N.; Banerjee, R. H<sub>2</sub>S and Its Role in Redox Signaling. *Biochim. Biophys. Acta - Proteins Proteomics* **2014**, *1844* (8), 1355–1366.
- (6) Singh, S.; Padovani, D.; Leslie, R. A.; Chiku, T.; Banerjee, R. Relative Contributions of Cystathionine  $\beta$ -Synthase and  $\gamma$ -Cystathionase to H<sub>2</sub>S Biogenesis via Alternative Trans-Sulfuration Reactions. *J. Biol. Chem.* **2009**, *284* (33), 22457–22466.
- (7) Chiku, T.; Padovani, D.; Zhu, W.; Singh, S.; Vitvitsky, V.; Banerjee, R. H<sub>2</sub>S Biogenesis by Human Cystathionine  $\gamma$ -Lyase Leads to the Novel Sulfur Metabolites Lanthionine and Homolanthionine and Is Responsive to the Grade of Hyperhomocysteinemia. *J. Biol. Chem.* **2009**, *284* (17), 11601–11612.
- (8) Shibuya, N.; Tanaka, M.; Yoshida, M.; Ogasawara, Y.; Togawa, T.; Ishii, K.; Kimura, H. 3-Mercaptopyruvate Sulfurtransferase Produces Hydrogen Sulfide and Bound Sulfane Sulfur in the Brain. *Antioxid. Redox Signal.* **2009**, *11* (4), 703–714.
- (9) Yadav, P. K.; Yamada, K.; Chiku, T.; Koutmos, M.; Banerjee, R. Structure and Kinetic Analysis of H<sub>2</sub>S Production by Human Mercaptopyruvate Sulfurtransferase. *J. Biol. Chem.* **2013**, *288* (27), 20002–20013.
- (10) Kabil, O.; Banerjee, R. Characterization of Patient Mutations in Human Persulfide Dioxygenase (ETHE1) Involved in H<sub>2</sub>S Catabolism. *J. Biol. Chem.* **2012**, *287* (53), 44561–44567.

- (11) Kabil, O.; Vitvitsky, V.; Banerjee, R. Sulfur as a Signaling Nutrient Through Hydrogen Sulfide. *Annu. Rev. Nutr.* **2014**, *34* (1), 171–205.
- (12) Hildebrandt, T. M.; Grieshaber, M. K. Three Enzymatic Activities Catalyze the Oxidation of Sulfide to Thiosulfate in Mammalian and Invertebrate Mitochondria. *FEBS J.* **2008**, *275* (13), 3352–3361.
- (13) Vitvitsky, V.; Yadav, P. K.; Kurthen, A.; Banerjee, R. Sulfide Oxidation by a Noncanonical Pathway in Red Blood Cells Generates Thiosulfate and Polysulfides. *J. Biol. Chem.* **2015**, *290* (13), 8310–8320.
- (14) Vitvitsky, V.; Yadav, P. K.; An, S.; Seravalli, J.; Cho, U.-S.; Banerjee, R. Structural and Mechanistic Insights into Hemoglobin-Catalyzed Hydrogen Sulfide Oxidation and the Fate of Polysulfide Products. *J. Biol. Chem.* **2017**, *292* (13), 5584–5592.
- (15) Bostelaar, T.; Vitvitsky, V.; Kumutima, J.; Lewis, B. E.; Yadav, P. K.; Brunold, T. C.; Filipovic, M.; Lehnert, N.; Stemmler, T. L.; Banerjee, R. Hydrogen Sulfide Oxidation by Myoglobin. *J. Am. Chem. Soc.* **2016**, *138* (27).
- (16) Ruetz, M.; Kumutima, J.; Lewis, B. E.; Filipovic, M. R.; Lehnert, N.; Stemmler, T. L.; Banerjee, R. A Distal Ligand Mutes the Interaction of Hydrogen Sulfide with Human Neuroglobin. *J. Biol. Chem.* **2017**, *292* (16).
- (17) Riedl, S. J.; Salvesen, G. S. The Apoptosome: Signalling Platform of Cell Death. *Nature Reviews Molecular Cell Biology.* 2007, pp 405–413.
- (18) Nicholls, P.; Kim, J. K. Oxidation of Sulphide by Cytochrome aa<sub>3</sub>. *Biochim. Biophys. Acta* **1981**, *637* (2), 312–320.
- (19) Wedmann, R.; Bertlein, S.; Macinkovic, I.; Böltz, S.; Miljkovic, J. L.; Muñoz, L. E.; Herrmann, M.; Filipovic, M. R. Working with “H<sub>2</sub>S”: Facts and Apparent Artifacts. *Nitric Oxide* **2014**, *41*, 85–96.
- (20) Koppenol, W. H.; Bounds, P. L. Signaling by Sulfur-Containing Molecules. Quantitative Aspects. *Arch. Biochem. Biophys.* **2017**, *617*, 3–8.
- (21) Battistuzzi, G.; Borsari, M.; Cowan, J. A.; Ranieri, A.; Sola, M. Control of Cytochrome c Redox Potential: Axial Ligation and Protein Environment Effects. *J. Am. Chem. Soc.*

- 2002**, 124 (19), 5315–5324.
- (22) Collman, J. P.; Ghosh, S.; Dey, A.; Decreau, R. A. Using a Functional Enzyme Model to Understand the Chemistry behind Hydrogen Sulfide Induced Hibernation. *Proc. Natl. Acad. Sci.* **2009**, 106 (52), 22090–22095.
- (23) Doeller, J. E.; Grieshaber, M. K.; Kraus, D. W. Chemolithoheterotrophy in a Metazoan Tissue: Thiosulfate Production Matches ATP Demand in Ciliated Mussel Gills. *J. Exp. Biol.* **2001**, 204 (0022–0949 (Print)), 3755–3764.
- (24) Hu, L.; Lu, M.; Wu, Z.; Wong, P. T.-H.; Bian, J. Hydrogen Sulfide Inhibits Rotenone-Induced Apoptosis via Preservation of Mitochondrial Function. *Mol. Pharmacol.* **2009**, 75 (1), 27–34.
- (25) Battistuzzi, G.; Borsari, M.; Dallari, D.; Lancellotti, I.; Sola, M. Anion Binding to Mitochondrial Cytochromes c Studied through Electrochemistry Effects of the Neutralization of Surface Charges on the Redox Potential. *Eur. J. Biochem.* **1996**, 241, 208–214.
- (26) Radi, R.; Thomson, L.; Rubbo, H.; Prodanov, E. Cytochrome c-Catalyzed Oxidation of Organic Molecules by Hydrogen Peroxide. *Arch. Biochem. Biophys.* **1991**, 288 (1), 112–117.
- (27) Alvarez-Paggi, D.; Hannibal, L.; Castro, M. A.; Oviedo-Rouco, S.; Demicheli, V.; Tórtora, V.; Tomasina, F.; Radi, R.; Murgida, D. H. Multifunctional Cytochrome c: Learning New Tricks from an Old Dog. *Chem. Rev.* **2017**, 117 (21), 13382–13460.
- (28) Mottley, C.; Mason, R. P.; Chignell, C. F.; Sivarajah, K.; Eling, T. E. The Formation of Sulfur Trioxide Radical Anion during the Prostaglandin Hydroperoxidase-Catalyzed Oxidation of Bisulfite (Hydrated Sulfur Dioxide). *J. Biol. Chem.* **1982**, 257 (9), 5050–5055.
- (29) Neta, P.; Huie, R. E. Free-Radical Chemistry of Sulfite. *Environ. Health Perspect.* **1985**, VOL. 64, 209–217.
- (30) Mottley, C.; Trice, T. B.; Mason, R. P. Direct Detection of the Sulfur Trioxide Radical Anion during the Horseradish Peroxidase-Hydrogen Peroxide Oxidation of Sulfite

- (Aqueous Sulfur Dioxide). *Mol. Pharmacol.* **1982**, *22*, 732–737.
- (31) Yadav, P. K.; Martinov, M.; Vitvitsky, V.; Seravalli, J.; Wedmann, R.; Filipovic, M. R.; Banerjee, R. Biosynthesis and Reactivity of Cysteine Persulfides in Signaling. *J. Am. Chem. Soc.* **2016**, *138* (1), 289–299.
- (32) Zhang, D.; MacInkovic, I.; Devarie-Baez, N. O.; Pan, J.; Park, C.-M.; Carroll, K. S.; Filipovic, M. R.; Xian, M. Detection of Protein S-Sulfhydration by a Tag-Switch Technique. *Angew. Chemie - Int. Ed.* **2014**, *53* (2).
- (33) Wedmann, R.; Onderka, C.; Wei, S.; Szijártó, I. A.; Miljkovic, J. L.; Mitrovic, A.; Lange, M.; Savitsky, S.; Yadav, P. K.; Torregrossa, R.; et al. Improved Tag-Switch Method Reveals That Thioredoxin Acts as Depersulfidase and Controls the Intracellular Levels of Protein Persulfidation. *Chem. Sci.* **2016**, *7* (5).
- (34) Buettner, G. R. The Pecking Order of Free Radicals and Antioxidants: Lipid Peroxidation,  $\alpha$ -Tocopherol, and Ascorbate. *Archives of biochemistry and biophysics.* 1993, pp 535–543.
- (35) Hammers, M. D.; Taormina, M. J.; Cerda, M. M.; Montoya, L. A.; Seidenkranz, D. T.; Parthasarathy, R.; Pluth, M. D. A Bright Fluorescent Probe for H<sub>2</sub>S Enables Analyte-Responsive, 3D Imaging in Live Zebrafish Using Light Sheet Fluorescence Microscopy. *J. Am. Chem. Soc.* **2015**, *137* (32), 10216–10223.
- (36) Le Trionnaire, S.; Perry, A.; Szczesny, B.; Szabo, C.; Winyard, P. G.; Whatmore, J. L.; Wood, M. E.; Whiteman, M. The Synthesis and Functional Evaluation of a Mitochondria-Targeted Hydrogen Sulfide Donor, (10-Oxo-10-(4-(3-Thioxo-3H-1,2-Dithiol-5-Yl)phenoxy)decyl)triphenylphosphonium Bromide (AP39). *Med. Chem. Commun.* **2014**, *5* (6), 728–736.
- (37) Arndt, S.; Baeza-Garza, C. D.; Logan, A.; Rosa, T.; Wedmann, R.; Prime, T. A.; Martin, J. L.; Saeb-Parsy, K.; Krieg, T.; Filipovic, M. R.; et al. Assessment of H<sub>2</sub>S in Vivo Using the Newly Developed Mitochondria-Targeted Mass Spectrometry Probe MitoA. *J. Biol. Chem.* **2017**, *292* (19), 7761–7773.
- (38) Garrido, C.; Galluzzi, L.; Brunet, M.; Puig, P. E.; Didelot, C.; Kroemer, G. Mechanisms

- of Cytochrome c Release from Mitochondria. *Cell Death and Differentiation*. 2006, pp 1423–1433.
- (39) Cai, J.; Yang, J.; Jones, D. P. Mitochondrial Control of Apoptosis: The Role of Cytochrome C. *Biochim. Biophys. Acta* **1998**, *1366* (1–2), 139–149.
- (40) Li, P.; Nijhawan, D.; Budihardjo, I.; Srinivasula, S. M.; Ahmad, M.; Alnemri, E. S.; Wang, X. Cytochrome c and dATP-Dependent Formation of Apaf-1/caspase-9 Complex Initiates an Apoptotic Protease Cascade. *Cell* **1997**, *91* (4), 479–489.
- (41) Luetjens, C. M.; Kögel, D.; Reimertz, C.; Düßmann, H.; Renz, A.; Schulze-Osthoff, K.; Nieminen, A.-L.; Poppe, M.; Prehn, J. H. M. Multiple Kinetics of Mitochondrial Cytochrome c Release in Drug-Induced Apoptosis. *Mol. Pharmacol.* **2001**, *60* (5).
- (42) Zou, H.; Yang, R.; Hao, J.; Wang, J.; Sun, C.; Fesik, S. W.; Wu, J. C.; Tomaselli, K. J.; Armstrong, R. C. Regulation of the Apaf-1/Caspase 9 Apoptosome by Caspase-3 and XIAP. *J. Biol. Chem.* **2002**, in press.
- (43) Kim, J.-E.; Tannenbaum, S. R. S-Nitrosation Regulates the Activation of Endogenous Procaspase-9 in HT-29 Human Colon Carcinoma Cells. *J. Biol. Chem.* **2004**, *279* (11), 9758–9764.
- (44) Mannick, J. B.; Schonhoff, C.; Papeta, N.; Ghafourifar, P.; Szibor, M.; Fang, K.; Gaston, B. S-Nitrosylation of Mitochondrial Caspases. *J. Cell Biol.* **2001**, *154* (6), 1111–1116.
- (45) Sivarajah, A.; Collino, M.; Yasin, M.; Benetti, E.; Gallicchio, M.; Mazzon, E.; Cuzzocrea, S.; Fantozzi, R.; Thiemeermann, C. Anti-Apoptotic and Anti-Inflammatory Effects of Hydrogen Sulfide in a Rat Model of Regional Myocardial I/R. *Shock* **2009**, *31* (3), 267–274.
- (46) Sen, N.; Paul, B. D.; Gadalla, M. M.; Mustafa, A. K.; Sen, T.; Xu, R.; Kim, S.; Snyder, S. H. Hydrogen Sulfide-Linked Sulfhydration of NF- $\kappa$ B Mediates Its Antiapoptotic Actions. *Mol. Cell* **2012**, *45* (1), 13–24.
- (47) Mitchell, D. A.; Morton, S. U.; Marletta, M. A. Design and Characterization of an Active Site Selective Caspase-3 Transnitrosating Agent. *ACS Chem. Biol.* **2006**, *1* (10), 659–

665.

- (48) Cuevasanta, E.; Lange, M.; Bonanata, J.; Coitiño, E. L.; Ferrer-Sueta, G.; Filipovic, M. R.; Alvarez, B. Reaction of Hydrogen Sulfide with Disulfide and Sulfenic Acid to Form the Strongly Nucleophilic Persulfide. *J. Biol. Chem.* **2015**, *290* (45).
- (49) Alexander, B. E.; Coles, S. J.; Fox, B. C.; Khan, T. F.; Maliszewski, J.; Perry, A.; Pitak, M. B.; Whiteman, M.; Wood, M. E.; Nakashima, I.; et al. Investigating the Generation of Hydrogen Sulfide from the Phosphoramidodithioate Slow-Release Donor GYY4137. *Med. Chem. Commun.* **2015**, *6* (9), 1649–1655.